Silicon Oxide Nanowire Growth Mechanisms Revealed by Real-Time Electron Microscopy

Miroslav Kolíbal[1,2], Libor Novák[3], Toby Shanley[4], Miloš Toth[4] and Tomáš Šikola[1,2]*

[1]Institute of Physical Engineering, Brno University of Technology, Technická 2, 616 69 Brno, Czech Republic

[2]CEITEC BUT, Brno University of Technology, Technická 10, 61669 Brno, Czech Republic

[3]FEI Company, Vlastimila Pecha 1282/12, 627 00 Brno, Czech Republic

[4]School of Mathematical and Physical Sciences, University of Technology, Sydney, Ultimo, 2007, Australia

*kolibal.m@fme.vutbr.cz

ABSTRACT

Growth of one-dimensional materials is possible through numerous mechanisms that affect nanowire structure and morphology. Here, we explain why a wide range of morphologies is observed when silicon oxide nanowires are grown on silicon substrates using liquid gallium catalyst droplets. We show that a gallium oxide overlayer is needed for nanowire nucleation at typical growth temperatures, and that it can decompose during growth and, hence, dramatically alter the nanowire morphology. Gallium oxide decomposition is attributed to etching caused by hydrogen that can be supplied by thermal dissociation of H_2O (a common impurity). We show that H_2O dissociation is catalyzed by silicon substrates at temperatures as low as 320 °C, identify the material supply pathways and processes that rate-limit nanowire growth in dry and wet atmospheres, and present a detailed growth model that explains contradictory results reported in prior studies. We also show that in wet atmospheres the Ga droplets can be mobile and promote nanowire growth as they traverse the silicon substrate.

GRAPHICAL ABSTRACT

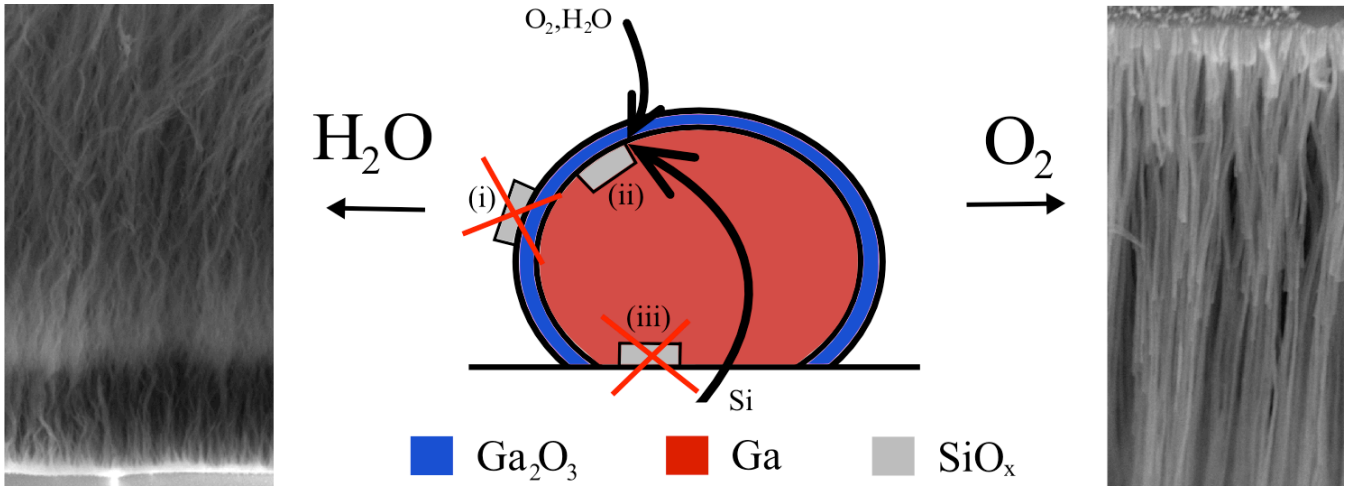

The root-growth mode of silicon oxide nanowires from a gallium catalyst is explained utilizing real-time in situ scanning electron microscopy.

KEYWORDS

Silicon oxide, nanowires, root growth, solid-liquid-solid growth, oxidation, gallium, gallium oxide, in-situ scanning electron microscopy

MANUSCRIPT TEXT

1. Introduction

Nanowires (NWs) and nanorods are an attractive class of nanostructured materials because they possess improved and new functionalities over their bulk counterparts. One-dimensional nanostructures have large surface-to-volume ratios that are beneficial for sensing, and a geometry that represents a promising new building block for devices.[1-4] Oxide nanowires possess many remarkable properties, and a large amount of knowledge is available on the functionality, chemistry and chemical modification of silica surfaces which can be used as active surfaces of sensors modified by various receptors, or biologically active composites that mimic enzyme activities.[10] The affinity of silica for biomolecules is increased further if substochiometric oxide compositions (SiO_x, where $x<2$) are realiazed.[11] Silicon oxide nanowires thus represent an ideal building block for photoactive,[12] sensing[13] and biosensing[14-16] devices with improved sensitivity over current state-of-the-art systems.[17,18]

Fabrication of nanowire-based devices requires a detailed understanding of NW growth mechanisms. The most investigated mechanism uses catalytic metal seeds to induce one-dimensional growth, and each specific process is denoted by the material pathway that leads to growth. For example, in vapor-liquid-solid growth (VLS) metallic droplets catalyse the decomposition of gaseous precursor molecules or act as collectors of diffusing adatoms. Nucleation is preferred at the solid/liquid interface between the droplet and the substrate[26] and nanowires grow with the droplet on top. However, due to thermodynamic limitations (the Gibbs-Thompson effect)[28] the growth of NWs with very small diameters (<10 nm) is extremely challenging.

In solid-liquid-solid (SLS) growth, the substrate material is dissolved in liquid droplets and precipitates on the droplet surfaces. It is common for multiple nanowires with small diameters (<20 nm) and extreme length (several millimeters)[41] to grow on top of each collector droplet.[53] Hence, SLS growth is a promising process for circumventing the Gibbs-Thompson effect.

Low-melting point metal catalysts are advantageous because they reduce nanowire growth temperatures. However, these materials oxidize under ambient conditions, which can alter or inhibit growth. Nevertheless, Sunkara et al. demonstrated the growth of silicon nanowires from molten Ga catalyst[39] and soon thereafter Pan et al.[40] and Zheng et al.[41] reported silicon oxide nanowires grown from Ga annealed at high temperature in an oxidative environment. The technique was subsequently utilized by other groups[42-46] using various low-melting-point catalysts.[47-52] Numerous nanowire morphologies have been demonstrated[56,57] such as dense bunches of nanowires that grow in from the catalyst particle,[40,41,46,56-58] and nanowire shells around the catalyst particles.[42,43] The particles are either pinned to the surface[42-44] or elevated above it.[45,46,56,57] The wide variety of observed morphologies is indicative of a complex growth mechanism. It is unclear whether the growth species diffuse through the droplet [59] or across the droplet surface,[44,60] or if supersaturation is reached in the gas phase or the liquid phase. The most compelling model of growth is based on the attachment of the growth species to nanowire roots that is preferred over the formation of new nuclei,[26,60] although other models have been proposed.[61]

Here, we use several experiments to elucidate the nanowire growth mechanism in the SiO_x (nanowire) – Ga (droplet) – Si(substrate) system. We show that the presence of water or hydrogen has a critical effect on the morphology of the growth products that we attribute to etching of a thin gallium oxide overlayer that typically forms on the catalyst particles during sample preparation. In the absence of water (or hydrogen), silicon oxide nanowires nucleate below the gallium oxide shell and grow towards the gallium core. However, when water (or hydrogen) is present in the system, the oxide shell is removed and nanowire bunches grow from the surface of each gallium droplet. Our experiments indicate that the oxide shell is necessary for nucleation and that the growth interface is located at the surface of the liquid metal catalyst, thus supporting the hypothesis that one-dimensional growth is driven by surface energy minimization during growth. Real-time electron imaging reveals the processes that rate-limit growth and provides direct evidence for the extreme mobility of Ga catalyst particles. Our results can likely explain the wide range of NW morphologies reported in the literature.

2. Experimental section

Sample preparation and nanowire growth. Nanowires were grown in two separate instruments. Most experiments were performed in an environmental reaction cell located inside a scanning electron microscope (SEM). The cell houses a gas cascade electron detector, a high temperature sample heater, capacitance manometer and is connected to a gas delivery system regulated by a mass-flow controller. The electron microscope chamber is pumped down to high vacuum (base pressure of 5×10^{-4} Pa) while SEM imaging is performed inside the reaction cell at gas pressures of up to 4 kPa. To prepare large Ga catalyst droplets, molten Ga was spread onto a piece of a Si wafer (both (111) and (100) orientations were used, with similar results), previously etched in buffered HF to remove the native silicon oxide. Samples were immediately loaded into the reaction chamber, pumped down to high vacuum, heated up to the desired growth temperature (200-930 °C) and the oxidizing gas was introduced (oxygen - purity 99.999%, nitrogen - purity 99.9%, or water vapor).

Gallium droplets and silicon oxide nanowires were also fabricated using an ultra-high vacuum (UHV, base pressure $<8\times10^{-8}$ Pa) cluster tool that allows in-situ Ga evaporation, exposure to controlled gaseous atmospheres (maximum pressure of 5×10^{-2} Pa) and analysis by X-ray photoelectron spectroscopy (XPS). Small Ga droplets (below 500 nm) were evaporated onto Si substrates under UHV conditions at different substrate temperatures (150-300 °C) to produce ensembles of Ga droplets with an uniform size.[63] The samples were either used for growth immediately or subsequently exposed to the ambient atmosphere to provide gallium oxide shell formation. After oxidation, the samples were used for growth in a SEM reaction chamber or reinserted into the UHV chamber.

XPS analysis of gallium oxide decomposition. XPS spectra of the clean samples were taken using Al Kα radiation (1486.6 eV) at an electron exit angle of 41° with respect to the surface plane. After XPS measurements, the sample was transferred under UHV conditions to another UHV chamber and exposed for 10 minutes to pure oxygen (99.999%) or water vapor at elevated temperature. The maximum

allowable pressure in the chamber is 6×10^{-2} Pa, which is significantly lower than the pressure during nanowire growth inside the SEM reaction chamber. Hence, to check for the relevance of these experiments, we have checked ex-situ that the nanowire growth proceeds also at these low pressures. Note that the XPS measurements were done after sample cooling from the reaction temperature. To avoid compromising the results by post-oxidation or thermal decomposition of the oxide, we performed sample cooling in both high vacuum and oxidizing atmospheres with similar results.

Real time Energy Dispersive X-Ray Spectroscopy measurements were performed in a similar microscope as the growth experiments, equipped with an EDX detector and a hot stage. Samples were prepared as for NW growth by spreading liquid Ga onto a buffered-HF etched Si substrate. They were annealed at 550 °C in high vacuum (5×10^{-3} Pa). The x-ray signal was excited using a 5 keV electron beam focused onto a large gallium droplet (10 μm in diameter) and detected in a 200 eV-energy window centered on 1.74 keV (Si Kα). The Monte Carlo code CASINO[64] was used to simulate the maximum x-ray generation depth in Ga, which is smaller than 200 nm at 5 keV. Hence, the x-ray signal was generated exclusively in the near-surface region of the catalyst droplet.

The growth products were also analyzed ex-situ by high resolution SEM, microscopic Fourier Transform Infrared Spectroscopy (FTIR) and cathodoluminescence spectroscopy.

3. Results and discussion

We analyzed the growth products by ex-situ, high resolution SEM. Representative images of structures grown for 10 minutes in dry and wet atmospheres (at 930 and 500 °C, respectively) are shown in Fig. 1. If a dry oxidative agent is used (nitrogen containing oxygen traces, Fig. 1a-c), the large Ga droplets are encapsulated by a thick porous shell. Closer inspection of the shell morphology is possible because it is usually cracked, revealing that the shell is made of nanowires (Fig. 1b). NW shells were observed to encapsulate Ga droplets with diameters ranging from several hundred nanometers to a millimeter, which is consistent with prior reports.[40,42,43,48,51] Chemical analysis confirms that the

nanowires consist of non-stoichiometric silicon oxide (see Supplementary Information S1 for details). A variety of structures was found after growth – catalyst droplets with a single nanowire shell (Fig. 1a), droplets with multiple, onion-like nanowire shells and complex, exotic, faceted multilayers (see Supplementary Information S2). Additional examples can be found in the literature.[40,49,50,56] Every Ga droplet with a nanowire shell has an etch pit at the base (see Fig. 1c and Supplementary Information S2), indicating that the substrate material was consumed during growth.[41-43,50] High resolution electron microscopy images show the presence of a very thin compact layer at the outer part of the shell (Fig. 1b,c). The presence of such a layer was also reported previously, and chemical analysis showed that it is composed mainly of Ga and O atoms.[40] We have examined this layer in more detail by site-selective cathodoluminescence measurements (see Supplementary information S3), showing that it is native Ga_2O_3 and below we will show that it plays a crucial role in promoting nanowire growth.

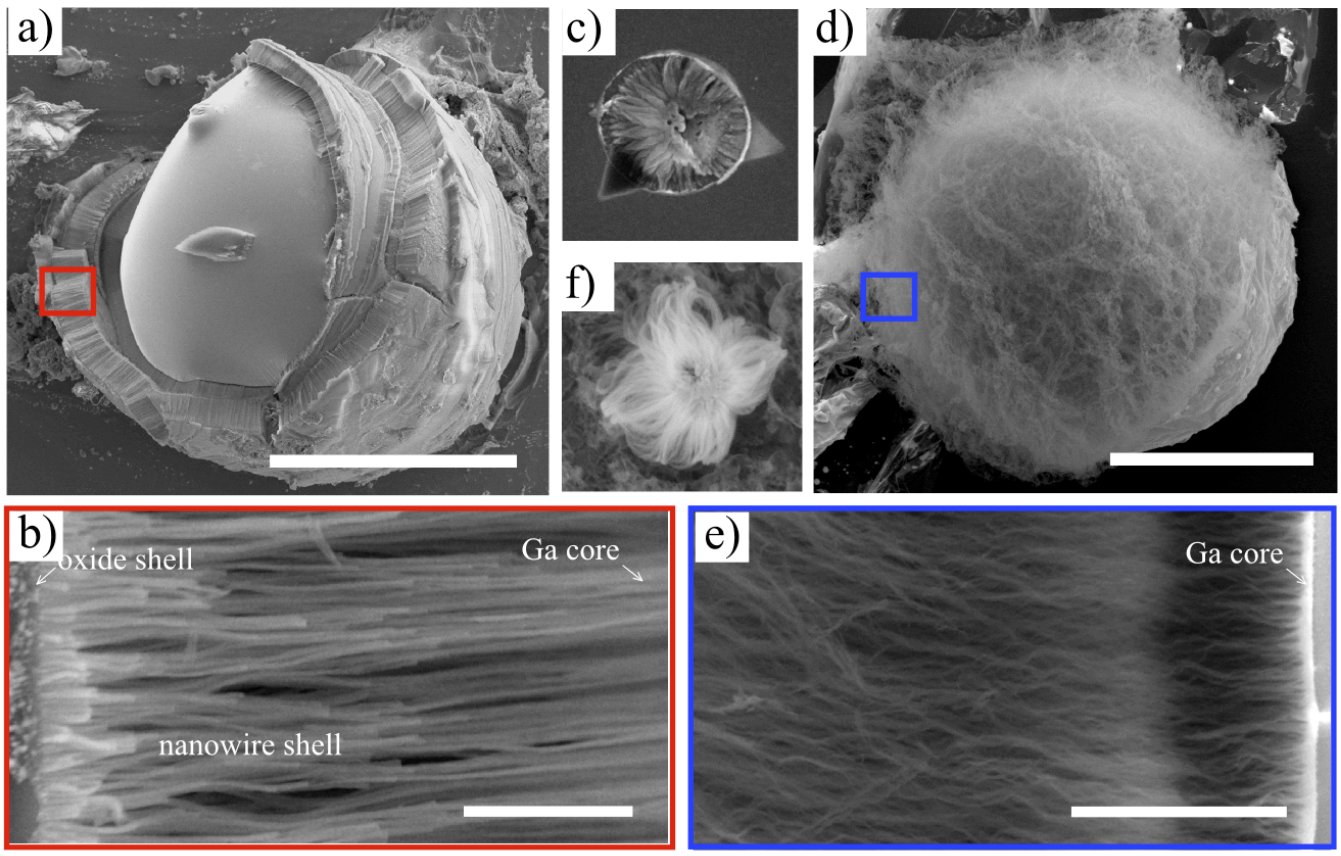

Fig.1: *a-c) Ex-situ SEM images of growth products fabricated in a dry oxidizing atmosphere at 600 Pa nitrogen and 930 °C. a) A large Ga droplet, exhibiting a thick shell made of silicon oxide nanowires;*

scale bar, 50 μm. b) Magnified image of the nanowire shell marked by a red rectangle in a); scale bar, 500 nm. c) Silicon oxide nanowires grown from a small catalyst droplet. Here, the Ga catalyst had an initial diameter of 300 nm. After growth, the Ga core is completely expelled from the droplet, and the remaining product consists of nanowires encapsulated by a gallium oxide shell. A triangular etch pit is clearly visible below the droplet. d-f) Ex-situ SEM images of growth products fabricated in a wet oxidizing atmosphere at 250 Pa of water vapor and 500 °C. d) A large Ga droplet, surrounded by dense bunches of silicon oxide nanowires; scale bar, 5 μm, e) Magnified image of the silicon oxide nanowires marked by a blue rectangle in d); scale bar, 500 nm, f) Nanowire bunches grown from a small Ga droplet (300 nm in diameter).

A very distinct nanowire morphology is observed if water vapor is introduced into the growth chamber. Unlike the highly-aligned nanowires grown in a dry oxidizing gas, water-oxidized NWs grow in bunches outwards from the surface of the catalyst droplet (Fig. 1d-f), and individual nanowires have a stranded morphology. This is observed even if very small (<300 nm) Ga droplets are used to catalyze the growth (Fig.1f). The etch pits below the catalyzing droplets are present, as in the case of a dry oxidizing gas (see Supplementary information S4). Notably, if the oxidizing atmosphere is not precisely controlled, both nanowire morphologies can be observed (see Supplementary Information S2). In this experiment, a small leak to the gas delivery system was introduced and, therefore, the nitrogen atmosphere (300 Pa) contained a small amount of water vapor.

The parameter window for nanowire growth is wide and similar for both dry and wet oxidation. Nanowires were successfully fabricated at temperatures in the range of 200 to 930 °C (higher temperatures were not tested). Growth was performed at pressures as high as 4 kPa (in the SEM reaction cell), and as low as 10^{-2} Pa (in the UHV chamber). The nanowire diameter (7-20 nm) is only slightly dependent on temperature, as predicted by theoretical models.[46,65] The nanowires grown in water vapor exhibit consistently smaller diameters than those grown in a dry atmosphere. The growth experiments in

the UHV chamber, where the gallium catalyst can be evaporated in-situ without exposure to ambient conditions (and so does not contain a native oxide), have resulted in the important conclusion that the gallium oxide is necessary for nanowire growth. Without the oxide shell, NW growth was not observed in a wet atmosphere and only occasionally in a dry atmosphere (where the re-oxidation of the catalyst can eventually take place).

NW growth in a dry atmosphere. The ex-situ inspection of the dry-oxidation growth products (Fig. 1b) shows that the nanowires grow between the native oxide shell and the gallium core. To elucidate the growth mechanism, we start by analyzing mass transport of the reactants to the growth interface. To unravel the silicon supply pathway, we measured the elemental composition of a catalyst droplet during annealing in high vacuum by in-situ Energy Dispersive X-ray Spectroscopy (EDX). The experimental conditions were chosen so as to excite the x-rays exclusively in the top 200 nm layer of a 10 μm catalyst droplet. The sample was heated to 550 °C and the Si-related signal started to increase immediately (see Supplementary information, Fig. S5), and saturated after a few minutes. Note that at this temperature evaporation of Si from the substrate is negligible and that NW growth was not observed (i.e. without introducing oxygen or water vapor). The increase in the Si-related x-ray signal can be explained by diffusion of Si across the catalyst surface (and subsequent diffusion into the Ga droplet through the gallium oxide shell), or direct diffusion of Si into the Ga droplet through the droplet/substrate interface. The former is unlikely as the nanowire density and length are independent of the gallium droplet size (Fig. 1a), and would be expected to cause NWs to nucleate on top of the oxide shell rather than the shell-Ga interface. Hence, silicon is likely dissolved in the liquid metal and diffuses through the droplet. Oxygen is supplied from the vapor phase. It likely diffuses through the gallium oxide shell and reacts with Si present in the Ga droplet, forming silicon oxide that causes SiO_x clusters to nucleate. Our experimental observation that NWs do not grow until the partial pressure of oxygen-containing molecules is significantly increased indicates that the SiO_x nanowires do not form through oxidation of precipitated Si.

Next, we analyze the growth kinetics using real-time in-situ electron microscopy.[68] The image sequence in Fig. 2a shows the most important processes occurring during growth in a dry oxidizing atmosphere. The first image shows a Ga droplet with a diameter of 2.7 μm after heating up to 860 °C. The subsequent images were taken in 2 second intervals. Although the images cannot be used to resolve individual nanowires, the growth of a nanowire shell and the movement of the growth front towards the liquid Ga core is clearly visible due to image contrast between the shell and the bright Ga core. The Ga core is compressed by the growing NWs and the core material is often expelled from the droplet towards the substrate or released by cracking of the nanowire shell. The former is documented by the image sequence shown in Fig. 2a, where a new layer (seen as a bright feature relative to the silicon substrate) is seen to form and propagate away from the Ga droplet as the Ga core disappears. Interestingly, a new Ga droplet appears at one point in the movie (the last image in the sequence). This has been observed in other experiments such as the case of Ga droplets on a carbon support.[69] We hypothesize that after reaching the solubility limit in Si, the gallium precipitates out as a droplet. The formation of these new Ga droplets is very frequent. Occasionally, we have observed Ga extrusions from cracks that form in the gallium oxide shell (similar to experiments with Ga lithiation),[70] but the former scenario was predominant, probably because the liquid Ga surface exposed to the oxygen-containing atmosphere is rapidly oxidized (see Supplementary Information S6). Diffusion into the substrate is the most likely pathway for the outward flow of Ga from catalyst droplets.

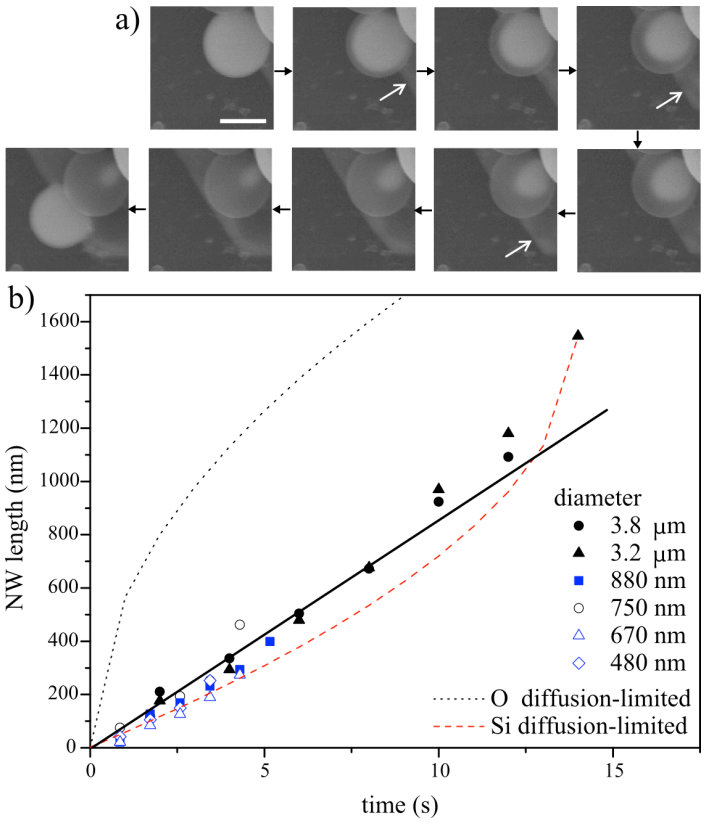

Fig. 2: *Real-time in-situ SEM observation of NW shell growth in a dry oxidizing atmosphere and associated growth kinetics. a) Image sequence obtained from a movie in 2 second steps, showing a disappearing Ga core (bright droplet) and a growing NW shell, as well as Ga expelled from the droplet (marked by the white arrows) during growth; scale bar, 2 µm. b) Dependence of the NW shell thickness on time at 860 °C for different initial droplet sizes and different oxidizing gases (scattered datapoints). Blue and black symbols represent data from experiments performed in oxygen and nitrogen atmospheres, respectively. The lines are fits (diffusion length calculated as* $\sqrt{Dt}$ *) to the experimental data from the 3.2 µm droplet (filled triangles) obtained using a diffusion-driven growth model – the black dotted line represents the oxygen-diffusion-limited regime (assuming a diffusion coefficient, D, of* 3.2×10^{-9} *cm*^{2}*/s for oxygen in* SiO_2 *at 860 °C),*[66] *the red dashed line represents the silicon-diffusion-limited regime (assuming that* $D = 1.4\times10^{-9}$ *cm*^{2}*/s for silicon diffusion in liquid Ga, which is in this case one order of magnitude lower than the value reported for 450 °C).*[67] *Note that the curves simulated for the oxygen and silicon-limited regimes have sublinear and superlinear dependencies on time, respectively, since the oxygen atom travel distance to the nucleation point increases as the NWs grow,*

while that of the silicon atoms decreases because of the shrinking gallium core.

Real-time microscopy allows us to quantify the nanowire growth rate using image sequences similar to that shown in Fig. 2a. The NW length is approximated by the distance between the outer surface of the shell and the shrinking Ga core (i.e. the thickness of the nanowire shell). The dependence of the nanowire length on time is shown in Fig. 2b for nanowires grown from Ga droplets of different sizes at 860 °C under both dry oxygen and nitrogen gas. The NW growth rate is not limited by the supply rate of oxygen molecules since the growth rate is the same in both oxygen and nitrogen atmospheres (and the latter cointained only a trace amount of oxygen). The growth rate is nearly constant (i.e. the NW legth scales linearly with time as shown by the straight line in Fig. 2b). Therefore, it is neither limited by oxygen diffusion along the growing NWs nor by silicon diffusion through the gallium droplet, both of which would have shown the $\sqrt{Dt}$ dependencies illustrated by dotted and dashed curves in Fig. 2b. Additionally, the latter scenario, i.e. silicon diffusion limited process, is inconsistent with the fact that the growth rate is independent of the initial size of the Ga droplet (within the range studied in our experiments). Hence, the growth rate is likely limited by (i) the reaction rate (Si oxidation) or (ii) the supply rate of oxygen via diffusion through the gallium oxide shell. The results in Fig. 2 cannot be used to deduce unambiguously the rate-limiting mechanism. However, additional experiments will be discussed below to show that scenario (ii) is more likely. Additionally, scenario (ii) is consistent with a subtle increase in growth rate observed during later stages of growth in several experiments (e.g. see Fig. 2b, data for Ga droplets with a diameter of 3.2 μm) due to gallium oxide shell thinning caused by water-assisted etching. The Arrhenius analysis of growth rates measured at different temperatures enables determination of the corresponding activation energy (see Supplementary Information S7).

NW growth in a wet atmosphere. Fig.1 indicates that growth induced by a wet oxidant (water vapor) is strikingly different. Nanowires grow outwards from the catalyst droplets, forming dense wool-like patterns. Fig. 3a shows an image sequence of growth from a Ga droplet at 410 °C under 200 Pa of

water vapor. Here, the quantitative analysis of the growth rate is less straightforward due to the stranded nanowire morphology, but key features of the growth process can still be derived from the experiment. Nanowire growth is initially accompanied by shrinkage of the Ga core, similarly to the case of growth in a dry atmosphere. However, during the later stages of growth, the gallium core ceases to shrink and nanowire bunches spread outwards from the Ga droplet. Notably, the oxide shell becomes detached from the Ga catalyst (marked by the arrows in Fig. 3a). Images of numerous growth products suggest that the gallium oxide shell is either etched away completely during growth (see Fig. 1f) or etched sufficiently to break up and detach from the catalyst droplet (Fig. 3a, Supplementary Information Fig. S4d). After some time, growth terminates (at ~342 s in the case documented in Fig. 3a) and does not resume. The growth termination is accompanied by a change in catalyst droplet image contrast.

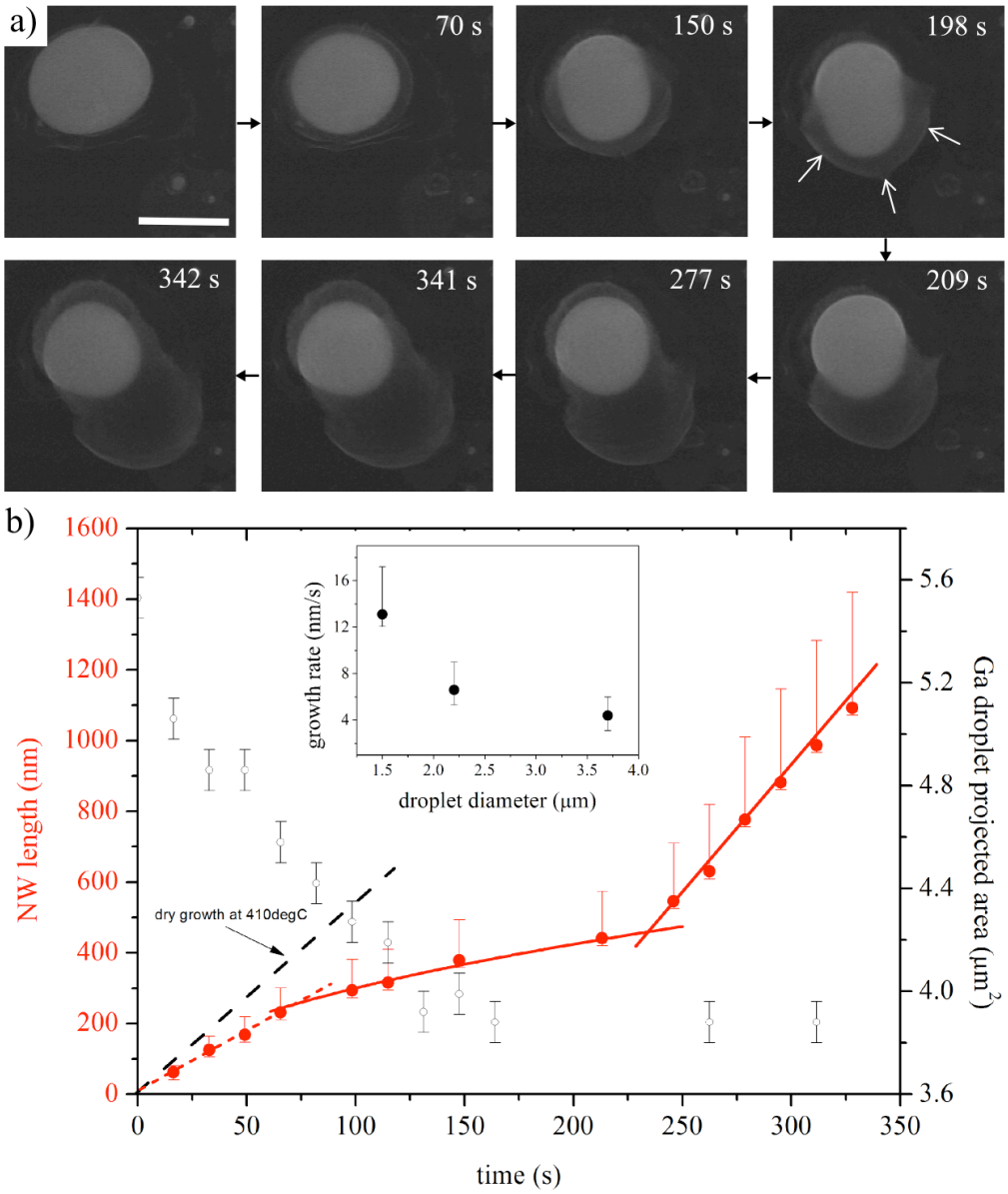

Fig. 3: *Real-time in-situ SEM observation of NW growth in a wet oxidizing atmosphere at 410 °C under 200 Pa of water vapor. a) Shortly after introduction of water vapor, the Ga core shrinks. The nanowires nucleate and grow towards the core (70 s). Subsequently, nanowire bunches grow outwards from the Ga catalyst, connected with what is possibly the remnant of the oxide shell (marked by the white arrows). The growth terminates at ~342 s and the Ga core abruptly becomes darker in the image (see images taken at 341 and 342 s); scale bar, 2 μm. b) Dependence of the NW growth rate on time at 410 °C for a Ga catalyst with an initial diameter of 2.6 μm (different from the one shown in (a)). The dashed black line shows the growth rate dependence measured at the same temperature in a dry*

atmosphere (Supplementary Information S7), while the red curves show three distinct stages of growth. The open circles show the calculated projected Ga catalyst area. Inset: dependence of the nanowire growth rate on the Ga core diameter measured during the final (third) stage of growth.

The quantitative analysis of growth in a wet atmosphere is limited by relatively large uncertainties in NW lengths estimated from real-time SEM images. Nevertheless, correlation of the data with ex-situ high-resolution SEM images enables assessment of the uncertainties and analysis of the data as shown in Fig. 3b. Growth in a wet atmosphere proceeds in three stages: (i) initially, the growth rate is constant, (ii) subsequently the growth rate significantly decelerates, and eventually (iii) rapidly accelerates. During stage (i) the gallium core shrinks as can be seen from the calculated projected Ga catalyst area shown in Fig. 3b, but the rate of shrinkage significantly decreases during stage (ii). The core dimensions (and volume) do not change during stage (iii). Hence, similarly to growth in a dry atmosphere, the NWs initially nucleate at the Ga/gallium oxide interface and grow towards the core. The initial growth rate is very similar to that in a dry atmosphere (see the dashed line in Fig. 3b), suggesting that it is limited by diffusion of water molecules through the gallium oxide shell, and that the associated diffusivity is similar in both atmospheres. The growth rate subsequently decreases and shows a sub-linear diffusion-limited behavior, indicating that the growth is limited by diffusion of water molecules along the NWs. The rapid increase of the growth rate in stage (iii) is related to the detachment of the remnants of the gallium oxide shell. Water molecules do not diffuse along the NWs to the growth interface anymore, but are instead supplied directly from the gas phase.[71] In this growth regime the growth rate depends inversely on the gallium droplet size (see inset of Fig. 3b) which indicates that the growth is now limited by silicon diffusion through the Ga catalyst.

Gallium oxide decomposition. Although the final morphology of NWs grown in dry and wet atmospheres is strikingly different, our analysis shows that the underlying mechanisms are very similar and the main difference is the presence/absence of the gallium oxide shell and its attachement/detachement with respect to the Ga droplet during the later stages of growth. To elucidate

the shell decomposition mechanism we characterized the oxide shell after exposure to dry oxygen and water vapor at elevated temperatures by in-situ XPS (see Methods). The evolution of the Ga 2p peak during annealing in dry oxygen (Fig. 4a) shows that the gallium oxide shell remains intact up to a very high temperature (860 °C). Conversely, annealing in water vapor causes significant oxide reduction, even at temperatures as low as 320 °C, and the disappearance of the gallium oxide-related photoelectron peak is accompanied by an increase in the intensity of the metallic Ga peak. The low-temperature oxide reduction is surprising since Ga_2O_3 is very stable up to high temperatures.

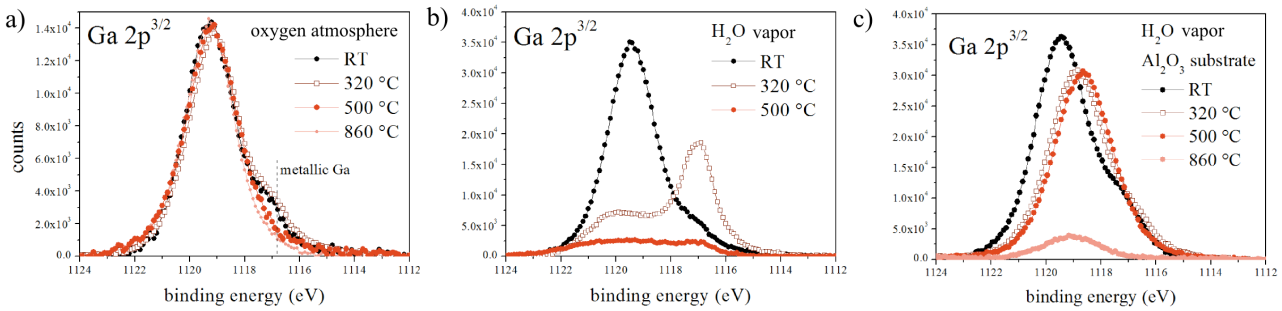

Fig. 4. *In-situ XPS analysis of the gallium oxide shell after exposure to different atmospheres at different temperatures. a) In pure oxygen, the oxide shell remains intact at annealing temperatures of 320, 500 and 860 °C. The intensity of the metallic Ga peak decreases at high temperatures due to oxide growth during annealing. b) In water vapor, the oxide-related peak and metallic Ga peak decreases and increases, respectively, due to decomposition of gallium oxide at temperatures as low as 320 °C. c) Importantly, annealing of oxide-encapsulated Ga droplets in water vapor on an alumina substrate does not result in decomposition of the gallium oxide shell at 320 or 500 °C, highlighting the critical role of silicon in the decomposition process.*

Gallium oxide is known to be reduced by molecular hydrogen via the following reactions:

$$Ga_2O_3 + 3H_2 \rightarrow 2Ga + 3H_2O,$$

$$Ga_2O_3 + 2H_2 \rightarrow Ga_2O + 2H_2O. \quad (1)$$

Indeed, we have also observed gallium oxide decomposition in a hydrogen atmosphere (similar to Fig. 4b, not shown here). However, there is no obvious source of hydrogen in our experimental setup,

particularly in the UHV cluster tool where the partial presure of hydrogen is extremely low. A possible pathway for the generation of hydrogen is the silicon oxidation reaction at an elevated temperature:

$$Si + 2H_2O \rightarrow SiO_2 + 2H_2. \quad (2)$$

To prove that silicon substrates play a role in the gallium oxide decomposition process, we prepared oxide-encapsulated Ga droplets on a Si substrate coated by 20 nm of Al_2O_3. Fig. 4c clearly shows that in water vapor the gallium oxide undergoes a significant decomposition only at temperatures higher than 500 °C (the peak shift is indicative of a stochiometric change towards Ga suboxides). Therefore, we conclude that silicon substrates act as catalysts for the decomposition of H_2O through reaction (2), generating H_2 that subsequently etches the gallium oxide shell during NW growth in a wet atmosphere.

Growth mode discussion. Our experiments show that the liquid-metal droplet mediates the diffusion of silicon to the growth front located at the droplet/NW interface. The oxidating species arrive from the vapor phase and are dissolved in the catalyst[72,73] where they react with Si (supplied from the solid phase via the solid-liquid interface). This implies that the oxidation of dissolved silicon must be preferred over catalyst oxidation. This condition is satisfied if the Gibbs free energy of the formation of the dissolved oxide is low compared to that of the metal droplet oxide (e.g. for silicon oxide it is very low compared to gallium oxide).[74]

Next, it is instructive to consider why the nanowires initially nucleate below the gallium oxide shell (Fig. 5a). Based on simple thermodynamic arguments nucleation is expected to be preferred on the outer surface of the gallium oxide (nucleus (i), Fig. 5), rather than the inner surface (nucleus (ii)), because of the very low surface free energy of silicon oxide (250-500 mJ/m^2 compared to the Ga/SiO_2 interface energy of 785 mJ/m^2).[46,75] However, our experiments indicate that nucleation at site (i) is limited by silicon diffusion through the gallium oxide shell. Hence, there are two interfaces where nucleation is likely - at the gallium oxide shell/Ga droplet interface (nucleus (ii)) or at the substrate/Ga droplet interface (nucleus (iii)). The Gibbs free energy change for these two cases is, however, similar (the surface free energies of Ga/Ga_2O_3 and Ga/Si interfaces are both between 0.7-0.8 mJ/m^2).[46,76] Hence,

there should be no preferential nucleation site, in contrast to our observation that nucleation is preferred below the oxide shell. We therefore conclude that the gallium oxide shell effectively lowers the energy barrier for the formation of SiO_x nuclei at position (ii). This is supported by the experimental observation that oxide NWs do not nucleate if the oxide shell is absent initially or during later stages of growth (Supplementary Information, Fig. S4d). It is noteworthy that the solubility of oxygen in Ga is a few orders of magnitude lower than that of Si.[77] Hence, supersaturation of Ga by SiO_x species occurs preferentially near the liquid-oxide shell interface, which highlights its importance as a preferential nucleation interface.[26,54]

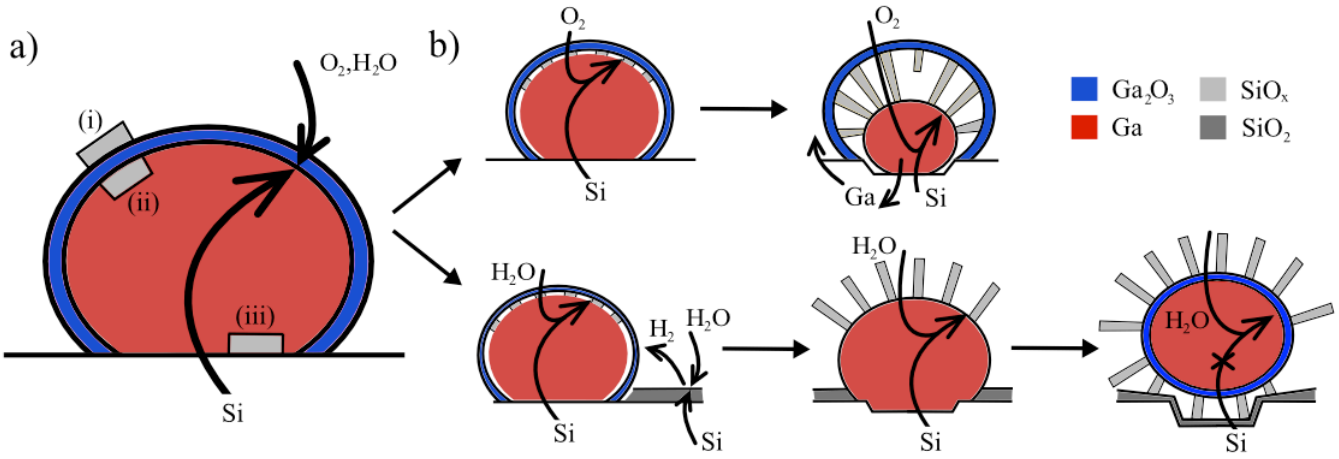

Fig. 5. *Schematic illustration of preferential nucleation (a) and material supply pathways (b) for silicon oxide nanowire growth in dry and wet oxidizing atmospheres. (a) Initial nucleation occurs at the liquid Ga/oxide shell interface (nucleus (ii)), minimizing the energy increase of the system. (b) In the case of dry oxidation (top) the gallium oxide shell is preserved and growth terminates if Ga is fully expelled from the droplet or if the outward flow of Ga is not possible. In the presence of water (or if hydrogen is supplied from an external source) the gallium oxide shell is etched away (bottom). Growth is fed by diffusion of the growth species to the nanowire base, and terminates if the Ga droplet is detached from the substrate. However, this can be prevented if the droplet moves across the surface (Supplementary Information S8), which results in almost unlimited supply of the growth material.*

NW growth in a dry atmosphere is illustrated schematically in Fig. 5b (top). Silicon atoms are supplied from the substrate and the growth rate is limited kinetically by diffusion of oxygen through the gallium oxide shell. Oxygen transport through the shell is mediated by the porous nature of the gallium oxide.[79] The growth front is at the NW-Ga interface and NW growth proceeds via attachment of the growth species to the nanowire base.

Nanowire growth in the presence of water vapor is mechanistically similar (Fig. 5b) during the initial stage of growth. However, the gallium oxide shell is continuously etched via reaction (1) by hydrogen generated through reaction (2). This explains why nanowires grow away from the catalyst surface, and not towards the core. The nanowires are no longer pinned to the gallium oxide shell and can therefore bend easily due to attractive forces[80,81] and form bunches (compared to those grown under the oxide shell).

Because the silicon substrate is readily oxidized by water at elevated temperatures, the Ga catalyst comes into contact with the growing silicon oxide. Gallium is known to decompose silicon dioxide[82] via the reactions

$$2Ga + SiO_2 \rightarrow SiO + Ga_2O,$$

$$4Ga + SiO_2 \rightarrow Si + 2Ga_2O. \qquad (3)$$

The gallium suboxide is decomposed by hydrogen, and gallium in the droplet is therefore not consumed during nanowire growth (in agreement with the experimental data shown in Fig. 3). Clearly, the reactions between gallium and silica show that the nanowires cannot be composed of pure SiO_2. Instead, non-stoichiometric oxides (SiO_x, $x<2$) which are not soluble in Ga were detected (Supporting Information S1 and S3), as in prior studies.[41,43-45,56,57]

If a Ga droplet looses contact with the silicon substrate, nanowire growth terminates because the Si supply path is broken and the Ga collector becomes depleted of silicon. This usually happens if the Ga droplet is elevated by a dense batch of nanowires (see Supporting Information, Fig. S4 and S8b). Oxidation of the underlying silicon substrate is no longer prevented by reaction (3) and local hydrogen formation via reaction (2) also decelerates (due to the absence of a Si surface). Consequently, the

formation of a gallium oxide shell on the Ga surface is promoted via water-induced oxidation. This is supported by the observed rapid change in Ga droplet contrast in SEM images (Fig. 3 and Supporting Information, Fig. S8) after growth termination, attributed to a change in the secondary electron yield caused by gallium oxide formation. Interestingly, real-time SEM revealed that, small Ga droplets are mobile in a wet atmosphere, and that the droplets continue to promote NW growth as they traverse the substrate (see Supporting Information S8). The movement acts to sustain reaction (3) because mobile droplets consume the silicon oxide along their paths. Finally, we note that immobile catalyst droplets can consume significant amounts of the underlying substrate material (see Supporting information, Fig. S4) via reactions (2) and (3).

Our model of growth in a water-containing atmosphere is applicable to numerous prior silicon oxide nanowire growth studies. Typically, hydrogen-containing carrier gases or precursors are used,[44,45,56,57] which effectively etch the gallium oxide yielding growth product morphologies that are similar to those observed here. Additionally, H_2O is a common impurity present as a gas contaminant or introduced through leaks in the system,[44,45,56] and is an additional source of hydrogen. If Si vapor or Si-containing molecules are supplied to the sample, nanowire growth does not cease when droplets detach from the substrate because the growth is fed by the Si atoms from the vapor, resulting in the "floating catalyst" morphology.[45,46,56,58] In the absence of hydrogen, the gallium oxide shell is present and the nanowires grow towards the catalyst core.[42,43]

4. Conclusions

We have demonstrated the critical role of gallium oxide in the growth of silicon oxide nanowires using liquid gallium catalyst droplets. The gallium oxide can decompose during growth, and thus alter the growth kinetics and nanowire morphology. The decomposition is caused by hydrogen which gives rise to etching, and can be supplied via thermal dissociation of H_2O, a common impurity in CVD systems. The dissociation of H_2O is catalyzed by silicon substrates at temperatures as low as 320 °C. We presented a detailed model of nanowire growth that accounts for both H-containing and H-free environments.

ELECTRONIC SUPPLEMENTARY INFORMATION

Electronic supplementary information (ESI) available: Additional nanowire analysis (Fig. S1-S4), real-time EDX analysis of Si content in the Ga droplet (Fig. S5), image sequence S6 showing crack formation and further evolution of the catalyst droplet morphology, determination of the activation energy of NW formation (Fig. S7), and a demonstration of Ga droplet migration (Fig. S8).

ACKNOWLEDGEMENTS

The authors acknowledge J. Čechal and P. Varga for critical reading of the manuscript. This work was supported by the Grant Agency of the Czech Republic (P108/12/P699) and by European Regional Development Fund – (CEITEC - CZ.1.05/1.1.00/02.0068). M. K. acknowledges the support of FEI Company.

REFERENCES

[1] Y. Cui and C. M. Lieber, *Science* 2001, 291, 851.

[2] C. Thelander, P. Agarwall, S. Brongersma, J. Eymery, L. F. Feiner, A. Forchell, M. Scheffler, W. Riess, B. J. Ohlsson, U. Gösele and L. Samuelson, *Mat. Today* 2006, 9, 28.

[3] H. Yan, H. S. Choe, S. Nam, Y. Hu, S. Das, J. F. Klemic, J. C. Ellenbogen and C. M. Lieber, *Nature* 2011, 470, 240.

[4] H. Riel, L. –E. Wernersson, M. Hong and J. A. del Alamo, *MRS Bull.* 2014, 39, 668.

[5] R. S. Wagner and W. C. Ellis, *Appl. Phys. Lett.* 1964, 4, 89.

[6] C. Gao, Q. Zhang, Z. Lu and Y. Yin, *J. Am. Chem. Soc*. 2011, 133, 19706.

[7] Y. Wu, J. Xiang, C. Yang, W. Lu and C. M. Lieber, *Nature* 2004, 430, 61.

[8] S. Park, J. Heo and H. J. Kim, *Nano Letters* 2011, 11, 740.

[9] J. Li, H. Z. Zhong, H. J. Liu, T. Y. Zhai, X. Wang, M. Y. Liao, Y. Bando, R. B. Liu and B. S. Zou, *J. Mat. Chem*. 2012, 22, 17813.

[10] Y. Tao, E. Ju, J. Ren and X. Qu, *Adv. Mater*. 2015, 27, 1097.

[11] M.-S. Hu, H.–L. Chen, C.-H. Shen, L.-S. Hong, B.-R. Huang, K.-H. Chen and L.-C. Chen, *Nature Mater*. 2006, 5, 102.

[12] S. Mukherjee, L. Zhou, A. M. Goodman, N. Large, C. Ayala-Orozco, Y. Zhang, P. Nordlander and N. J. Halas, *J. Am. Chem. Soc*. 2014, 136, 64.

[13] A. Rao, A. Bankar, A. Shinde, A. R. Kumar, S. Gosavi and S. Zinjarde, *ACS Appl. Mater. Interfaces* 2012, 4, 871.

[14] E. Murphy-Perez, S. K. Arya and S. Bhansali, *Analyst* 2011, 136, 1686.

[15] N. S. Ramgir, A. Zajac, P. K. Sekhar, L. Lee, T. A. Zhukov and S. Bhansali, *J. Phys. Chem. C* 2007, 111, 13981.

[16] P. K. Sekhar, N. S. Ramgir and S. Bhansali, *J. Phys. Chem. C* 2008, 112, 1729.

[17] A. Kausnik, R. Kumar, E. Huey, S. Bhansali, N. Nair and M. Nair, *Microchim Acta* 2014, 181, 1759.

[18] L. Tong, J. Lou, R. R. Gattass, S. He, X. Chen, L. Liu and E. Mazur, *Nano Letters* 2005, 5, 259.

[19] S. M. Prokes and S. Arnold, *Appl. Phys. Lett*. 2005, 86, 193105.

[20] C. X. Zhao, Y. F. Li, J. Zhou, L. Y. Li, S. Z. Deng, N. S. Xu and J. Chen, *Cryst.Growth Des*. 2013, 13, 2897-2905.

[21] W. Shim, J. Ham, K.-I. Lee, W. Y. Jeung, M. Johnson and W. Lee, *Nano Letters* 2009, 9, 18-22.

[22] D. Rudolph, S. Hertenberger, S. Bolte, W. Paosangthong, D. Spirkoska, M. Döblinger, M. Bichler, J. J. Finley, G. Abstreiter and G. Koblmüller, *Nano Letters* 2011, 11, 3848-3854.

[23] V. Consonni, M. Knelangen, L. Geelhaar, A. Trampert and H. Riechert, *Phys. Rev. B* 2010, 81, 085310.

[24] K. A. Bertness, A. Roshko, L. M. Mansfield, T. E. Harvey and N. A. Sanford, *J. Cryst. Growth* 2008, 310, 3154-3158.

[25] M. J. Bierman, Y. K. Albert Lau, A. V. Kvit, A. L. Schmitt and S. Jin, *Science* 2008, 320, 1060.

[26] B. A. Wacaser, K. A. Dick, J. Johansson, M. T. Borgström, K. Deppert and L. Samuelson, *Adv. Mater*. 2009, 21, 153.

[27] M. G. Jenke, D. Lerose, C. Niederberger, J. Michler, S. Christiansen and I. Utke, *Nano Letters* 2011, 11, 4213-4217.

[28] V. Schmidt, J. Wittemann and U. Gösele, *Chem. Rev*. 2010, 110, 361-388.

[x] H. F. Yan, Y. J. Xing, Q. L. Hang, D. P. Yu, Y. P. Wang, J. Xu, Z. H. Xi and S. Q. Feng, *Chem. Phys. Lett*. 2000, 323, 224.

[x2] C.-Y. Wang, L.-H. Chan, D.-Q. Xiao, T.-C. Lin and H. C. Shih, *J. Vac. Sci. Technol. B* 2006, 24, 613.

[29] M. C. Putnam, M. A. Filler, B. M. Kayes, M. D. Kelzenberg, Y. Guan, N. S. Lewis, J. M. Eiler and H. A. Atwater, *Nano Letters* 2008, 8, 3109-3113.

[30] J. E. Allen, E. R. Hemesath, D. E. Perea, J. L. Lensch-Falk, Z. Y. Li, F. Yin, M. H. Gass, P. Wang, A. L. Bleloch, R. E. Palmer and L. J. Lauhon, *Nature Nanotechnology* 2008,3, 168-173.

[31] O. Moutanabbir, D. Isheim, H. Blumtritt, S. Senz, E. Pippel and D. N. Seidman, *Nature* 2013, 496, 78-82.

[32] E. Koren, G. Elias, A. Boag, E. R. Hemesath, L. J. Lauhon and Y. Rosenwanks, *Nano Letters* 2011, 11, 2499-2502.

[33] P. Nguyen, H. T. Ng and M. Meyyappan, *Adv. Mater*. 2005, 17, 1773.

[34] K. A. Dick and P. Caroff, *Nanoscale* 2014, 6, 3006.

[35] G. V. Bianco, M. M. Giangregorio, P. Capezzuto, M. Losurdo, T.–H. Kim, A. S. Brown and G. Bruno, *Mat. Sci. Eng. B* 2012, 177, 700.

[36] F. Iacopi, P. M. Vereecken, M. Schaekers, M. Caymax, N. Moelans, B. Blanpain, O. Richard, C. Detavernier and H. Griffiths, *Nanotechnology* 2007, 18, 505307.

[37] I. Zardo, L. Yu, S. Conesa-Boj, S. Estradé, P. J. Alet, J. Rossler, M. Frimmer, P. Roca I Cabarrocas, F. Peiro, J. Arbiol, J. R. Morante, A. Fontcuberta i Morral, *Nanotechnology* 2009, 20, 155602.

[38] V. A. Nebol'sin and A. A. Shchetinin, *Inorg. Mater*. 2003, 39, 899.

[39] M. K. Sunkara, S. Sharma, R. Miranda, G. Lian and E. C. Dickey, *Appl. Phys.Lett*.2001, 79, 1546.

[40] Z. W. Pan, Z. R. Dai, C. Ma and Z. L. Wang, *J. Am. Chem. Soc*. 2002, 124, 1817.

[41] B. Zheng, Y. Wu, P. Yang and J. Liu, *Adv. Mater*. 2002, 14, 122.

[42] L. Dai, L. P. You, X. F. Duan, W. C. Lian and Q. Q. Qin, *Phys. Lett. A* 2005, 335, 304-309.

[43] P. A. Hu, Y. Q. Liu and X. B. Wang, *Appl. Phys. A* 2003, 77, 743-745.

[44] S. Luo, W. Zhou, W. Chu, J. Shen, Z. Zhang, L. Liu, D. Liu, Y. Xiang, W. Ma and S. Xie, *Small* 2007, 3, 444-450.

[45] X. Q. Yan, W. Y. Zhou, L. F. Sun, Y. Gao, D. F. Liu, J. X. Wang, Z. P. Zhou, H. J. Yuan, L. Song, L. F. Liu, G. Wang and S. S. Xie, *J. Phys. Chem. Solids* 2005, 66, 701-705.

[46] M. Bettge, S. MacLaren, S. Burdin, D. Abraham, I. Petrov, M.-F. Yu and E. Sammann, *J. Mater. Res*. 2011, 26, 2247.

[47] P. Wu, X. Zou, L. Chi, Q. Li and T. Xiao, *Nanotechnology* 2007, 18, 125601.

[48] R. Ma and Y. Bando, *Chem. Phys. Lett*. 2003, 377, 177-183.

[49] X. M. Cai, A. B. Djuriši and M. H. Xie, *J. Appl. Phys*. 2005, 98, 074313.

[50] J. Zhang, Y. Yang, S. Ding, J. Li and X. Wang, *Mat. Sci. Eng. B* 2008, 150, 180-186.

[51] J. Zhang, F. Jiang, Y. Yang and J. Li, *J. Cryst. Growth* 2007, 307, 76.

[52] J. Qu, Z. Zhao, X. Wang, J. Qiu, Y. Gogotsi, *Mater. Express* 2012, 2, 157.

[53] G. A. Bootsma and H. J. Gassen, *J. Cryst. Growth* 1971, 10, 223.

[54] K. W. Kolasinski, *Curr. Opinion in Solid State and Mat. Sci.* 2006, 10, 182.

[55] D. S. Kim, L. Scholz, U. Gösele and M. Zacharias, *Small* 2008, 4, 1615.

[56] Z. Pan, S. Dai, D.B. Beach and D. H. Lowndes, *Nano Letters* 2003, 3, 1279-1284.

[57] X. Zhang, Z. Liu, Z. Zheng and S. Hark, *J. Mater. Res.* 2008, 23, 1667.

[58] Z. Gu, F. Liu, J. Y. Howe, M. Parans Paranthaman and Z. Pan, *Nanoscale* 2009, 1, 347.

[59] H. F. Yan, Y. J. Xing, Q. L. Hang, D. P. Yu, Y. P. Wang, J. Xu, Z. Xi and S. Q. Feng, *Chem. Phys. Lett.* 2000, 323, 224-228.

[60] I. Aharonovich, Y. Lifshitz and S. Tamir, *Appl. Phys. Lett.* 2007, 90, 263109.

[61] D. Zhang and R. Q. Zhang, *J. Phys. Chem. B* 2006, 110, 1338.

[62] Q. X. Liu, C. X. Wang, N. S. Xu and G. W. Yang, *Phys. Rev. B* 2005, 72, 085417.

[63] M. Kolibal, T. Cechal, E. Brandejsova, J. Cechal and T. Sikola, *Nanotechnology* 2008, 19, 475606.

[64] D. Drouin, A. R. Couture, D. Joly, X. Tastet, Z. Aimez and R. Gauvin, *Scanning* 2007, 29, 92.

[65] H. Chandrasekaran, G. U. Sumanasekara and M. K. Sunkara, *J. Phys. Chem. B* 2006, 110, 18351.

[66] K. Kajihara, T. Miura, H. Kamioka, M. Hirano, L. Skuja and H. Hosono, *J. Ceram. Soc. Jap.* 2004, 112, 559.

[67] H. Ogawa, Q. Guo, K. Ohta, *J. Cryst. Growth* 1995, 155, 193.

[68] F. M. Ross, *Rep. Prog. Phys.* 2010, 73, 114501.

[69] S. Kodambaka, C. Ngo, J. Palisaitis, P. H. Mayrhofer, L. Hultman and P. O. A. Persson, *Appl. Phys. Lett.* 2013, 102, 161601.

[70] W. Liang, L. Hong, H. Yang, F. Fan, Y. Liu, H. Li, J. Li, J. Y. Huang, L.-Q. Chen, T. Zhu and S. Zhang, *Nano Letters* 2013, 13, 5212.

[71] O. A. Louchev, Y. Sato and H. Kanda, *Appl. Phys. Lett.* 2002, 80, 2752.

[72] H. Y. Dang, J. Wang and S. S. Fan, *Nanotechnology* 2003, 14, 738.

[73] L. Yu, B. O'Donnell, P. J. Alet, S. Conesa-Boj, F. Peiro, J. Arbiol and P. Roca i Cabarrocas, *Nanotechnology* 2009, 20, 225604.

[74] T. B. Reed, Free Energy of Formation of Binary Compounds: An Atlas of Charts for High-Temperature Chemical Calculations, The MIT Press, Cambridge, Mass. 1971

[75] Y. I. Tarasevich, *Theor. Exp. Chem.* 2006, 42, 145.

[76] S. Conesa-Boj, I. Zardo, S. Estrade, L. Wei, P. J. Alet, P. Roca i Cabarrocas, J. R. Morante, F. Peiro, A. Fontcuberta i Morral and J. Arbiol, *Cryst. Growth Des.* 2010, 10, 1534.

[77] C. B. Alcock and K. T. Jacob, *J. Less. Comm. Met.* 1977, 53,211.

[78] S. M. Roper, S. H. Davis, S. A. Norris and A. A. Golovin, *J. Appl. Phys.* 2007, 102, 034304.

[79] A. Plech, U. Klemradt, H. Metzger and J. Peisl, *J. Phys. Cond. Mat.* 1998, 10, 971.

[80] C. N. Cochran and L. M. Foster, *J. Electrochem. Soc.* 1962, 109, 149.

[81] Z. Sun, D. Wang and J. Xiang, *ACS Nano* 2014, 8, 11261.

[82] M. Khorasaninejad, N. Abedzadeh, A. S. Jawanda, O. Nixon, M. P. Anantram and S. S. Saini, *J. Appl. Phys.* 2012, 111, 044328.

[83] K. Ostrikov, I. Levchenko, U. Cvelbar, M. Sunkara and M. Mozetic, *Nanoscale* 2010, 2, 2012

[84] K. Ostrikov, D. H. Seo, H. Mehdipour, Q. Cheng and S. Kumar, *Nanoscale* 2012, 4, 1497.